Interface Properties of Metal/Graphene Heterostructures Studied by Micro-Raman Spectroscopy

ARTICLE *in* THE JOURNAL OF PHYSICAL CHEMISTRY C · NOVEMBER 2010

Impact Factor: 4.77 · DOI: 10.1021/jp106188w

6 AUTHORS, INCLUDING:

Yoshihito Maeda
Kyushu Institute of Technology
156 PUBLICATIONS **2,175** CITATIONS

Japanese Journal of Applied Physics **50** (2011) 04DN03 **REGULAR PAPER**
DOI: 10.1143/JJAP.50.04DN03

Interface Properties of Ag and Au/Graphene Heterostructures Studied by Micro-Raman Spectroscopy

Shiro Entani[1], Seiji Sakai[1], Yoshihiro Matsumoto[1], Hiroshi Naramoto[1], Ting Hao[1], and Yoshihito Maeda[1,2]

[1]*Advanced Science Research Center, Japan Atomic Energy Agency, Tokai, Ibaraki 319-1195, Japan*
[2]*Department of Energy Science and Technology, Kyoto University, Kyoto 606-8501, Japan*

Received September 21, 2010; accepted November 1, 2010; published online April 20, 2011

We have studied the influence of the interface formation of graphene with noble metals (Ag and Au) on its vibrational properties by using confocal micro-Raman spectroscopy. The interactions at the metal/graphene interface are investigated by comparing the results from two different regions, the heterostructure and pristine graphene regions, with and without noble metals on the same graphene sheet. In Ag/graphene, the Raman signal intensity was increased by the surface enhanced Raman scattering process, and the enhanced signals are found to be composed of the broadened D and G peak components emitted from the Ag/graphene interface. The precise evaluation of graphene-layer-number-dependence of the D and G bands revealed that the disordered graphitic carbons were adhered on the glass substrate during the sample preparation by the micromechanical cleavage method. In the 2D band, no obvious peak shift induced by the heterostructure formation was observed in Ag/graphene, whereas a large shift (more than $\sim$15 cm^{-1}) was observed at Au/single layer graphene. This is considered to be due to the difference in the amount of the doped carriers in graphene between two heterostructures.

1. Introduction

Graphene has attracted worldwide attention as one of the most promising materials for realizing nano-electronic and spintronic devices in recent years, due to the novel electronic and electric properties (e.g., quantum electronic transport, characteristic charge carriers which behave as massless Dirac fermions, a tunable band gap, and long spin-diffusion length).[1–4] In the devices using graphene, the elucidation and control of the charge injection process and the electronic structure at the interface between the graphene sheet and a metal electrode are essential for designing device properties.[5,6] Plenty of studies have been reported on the interactions at the interfaces in the metal/graphene heterostructures both theoretically and experimentally.[7–12] It has been theoretically demonstrated that the interactions between graphene and metals are strong enough to modify the π bands of graphene in the case of ferromagnetic metals (Co and Ni) and, on the other hand, negligibly weak in the case of noble metals (Au, Ag, and Cu). In contrast, some experimental studies have suggested that there are the non-ignorable interface interactions which modify the electronic structure of graphene in the Au-graphene heterostructure.[7,13] On the noble metal surfaces, surface enhanced Raman scattering (SERS) is expected to appear and it can provide a spectrum intensity enhancement of graphene up to $\sim$10 orders of magnitude.

In this study, interface-related phenomena of graphene in the noble metal/graphene heterostructures are investigated for the samples fabricated by metal deposition (Ag and Au) and with various graphene layers numbers, n (n = 1–5), by employing confocal micro-Raman spectroscopy considering the following two issues. The first issue is the size problem, that is the size of the graphene sheet fabricated with the micromechanical cleavage method is limited to less than 10's μm and additionally the size of the region with the same graphene layers number is around several μm typically. Micro-Raman spectroscopy is one of the most powerful techniques to investigate the chemical interactions and electronic structures of graphene by probing the vibrational property at a selected spot of less than about 1 μm.[14–16] It is known that three prominent bands appear in the Raman spectrum of graphene: the G band around 1580 cm^{-1}, the D band around 1360 cm^{-1} and the 2D (G′) band around 2700 cm^{-1}. The G band is ascribed to the doubly degenerate transverse (TO) and longitudinal (LO) optical phonon mode at the Brillouin zone center, which corresponds to the in-plane vibration of carbon atoms with E_{2g} symmetry. The D band is due to the TO phonons branches around the K point and requires the symmetry lowering for its activation, and is usually related to defects and structural distortions.[17] Thus, the D band provides the information on the perfection of the graphitic structure, and is not generally observed in the as-prepared graphene sheets by the micromechanical cleavage method. The 2D band is the overtone of the D band and is Raman active without the distortions different from the D band. The 2D band provides the information on the electronic structure of graphene through the double resonance process. These Raman bands also provide the information on the carrier (electron/hole) doping in graphene. It has been demonstrated that the carrier doping induced by the field-effect can be detected from the up-shift and down-shift behaviors of the G and 2D bands.[18–20] The 2D band is up-/down-shifted by the hole/electron doping, respectively. In contrast, the G band is up-shifted by both electron and hole doping due to the nonadiabatic removal of the Kohn anomaly at the zone center.[21,22] One can thus evaluate the type and amount of doping from the changes in the Raman peak positions. The second issue is the unintentional doping to the graphene sheet. Casiraghi *et al.* have pointed out that an unintentional hole doping to graphene occurs inhomogeneously even within the same graphene sheet, judging from the large variations of the Raman parameters depending on the position of the probing laser spot.[23] It is, therefore, necessary to exclude the influences of the unintentional doping on the Raman parameters for discussing the spectroscopic changes induced by metal deposition properly. For this purpose, we fabricated specially arranged specimens composed of the two different regions; the metal/graphene heterostructure region and the pristine graphene region on the same graphene sheet with the same graphene layers numbers, by using the micrometer patterned metal deposition with a shadow mask.

2. Experiment

Figure 1 shows an optical micrograph of the Ag/graphene

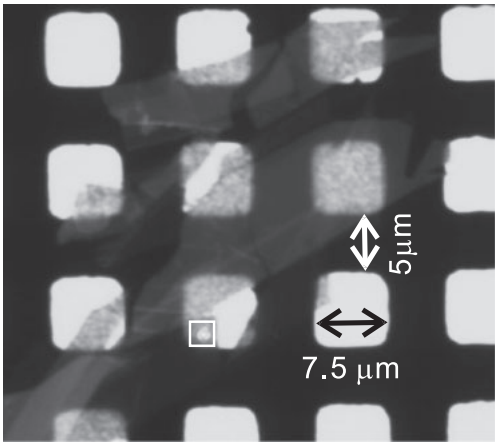

Fig. 1. An optical micrograph of Ag/graphene fabricated on a glass substrate. The graphene sheet is partially covered with the Ag films. The graphene sheet contains several areas with different layers numbers. A bright dot surrounded by the solid line indicates the probing laser spot for Raman measurements.

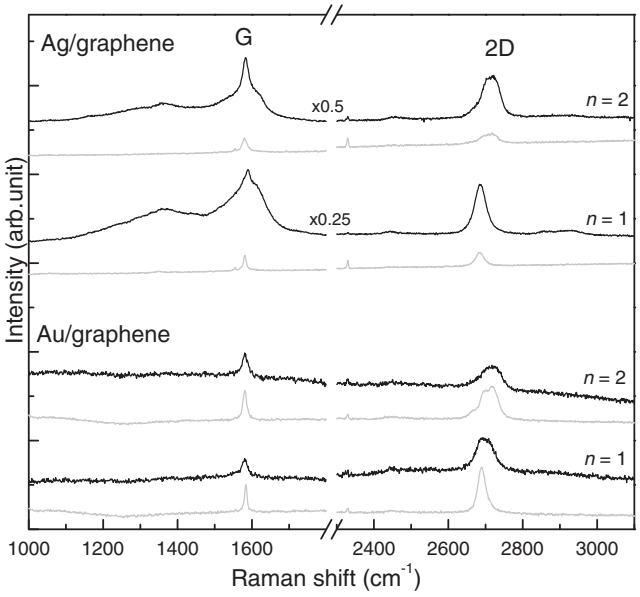

Fig. 2. A pair of the Raman spectra in the D, G, and 2D band regions obtained from the Ag/graphene and Au/graphene heterostructure regions and the pristine graphene regions with different graphene layers number of one and two, respectively.

sample (10 nm-Ag/graphene/glass) composed of the two regions of the metal/graphene heterostructure and pristine graphene. The fabrication procedures and the microstructures of the metal/graphene samples were mentioned elsewhere.[13] In short, graphene sheet was transferred onto a bolosilicate cover glass (Matsunami Glass, flatness < 0.010 mm, JIS R3702) by microcleaving highly oriented pyrolitic graphite (HOPG).[24] In this paper, the graphene layers number, n, in the cleaved graphene sheet is determined through the following procedures: In the case of thin graphene ($n = 1$–3), the layers number can be estimated by the component analysis of the 2D band.[17] The graphene sheet consists of the stacks of the patch-like thin graphene, as can be seen in Fig. 1. The thin graphene area extending from the thick graphene stacks region can be observed occasionally around the outer periphery of the graphene sheet. In the thick graphene ($n = 4$ and 5), therefore, the evaluation was made successfully by counting the graphene layers number from the stacks of the patch-like thin graphene with $n = 1$–3, by comparing the results from Raman spectroscopy and optical microscopy. The validity of this evaluation was confirmed by the linear increase of the G band intensity with the layers number increase in the confocal Raman spectra. The prepared substrate (graphene/glass) was introduced into an ultrahigh vacuum (UHV) chamber with a base pressure of 3×10^{-7} Pa and was annealed at 423 K for 1 h for degassing, and then the metal/graphene heterostructure was fabricated on a part of the graphene sheet by depositing a thin film (5–10 nm thick) of metals (Ag and Au) through a micro-patterned shadow mask. The metals were evaporated from the electron beam evaporator (Ag) and alumina coated tungsten basket (Au), respectively. The temperature of the glass substrate was kept at ambient temperature during the meal deposition. According to these procedures, we obtained the metal/graphene sample as shown in Fig. 1, which is composed of the two kinds of regions; the heterostructure regions (bright regions in the image) with a square shape of $7.5 \times 7.5\,\mu m^2$ arranged at a separate distance of 5 μm and the intermediate region of pristine graphene (dark regions in the image). The Raman measurements were carried out with a micro-Raman system (Tokyo Instruments NANO-FINDER) in a confocal backscattering geometry. Raman spectra were obtained by focusing Ar-ion laser (488 nm, 1 mW) to the selected spots with less than 1 μm diameter on the sample surface under ambient condition. The spectral resolution of the spectrometer was about $3\,cm^{-1}$. For the measurements of the heterostructure regions, Raman spectra were obtained through the metal film layer. The deposition thicknesses of metals in the samples for the Raman measurements are 10 nm for Ag and 5 nm for Au, respectively, and are thin enough for laser penetration and detection of the Raman signals through the metal layer. The micro-scale patterned structure of the metal/graphene specimen enables us to investigate the graphene layers number, n, dependences of the Raman parameters simply by changing the probing position on the graphene sheet, since each sheet contains several regions with different layers numbers as seen as the laminar contrast variation in the image of the graphene sheet in Fig. 1. Changes in the Raman parameters; peak positions and the full width at the half maximum (FWHM) of the D, G, and 2D bands, due to the formation of the metal/graphene heterostructure are examined by comparing a pair of the Raman spectra obtained at the neighboring two spots in the heterostructure and pristine graphene regions which are separated by within 2–3 μm.

3. Results and Discussion

Figure 2 shows Raman spectra of Ag/graphene and Au/graphene with the graphene layers of one and two. In this figure, the data consist of pairs of two spectra obtained at the heterostructure region (black line) and at the pristine graphene region (gray line) within the same graphene sheet with the identical graphene layers number as mentioned above. It is found that, in the heterostructure regions, the respective peaks exhibit shifts of the peak positions and

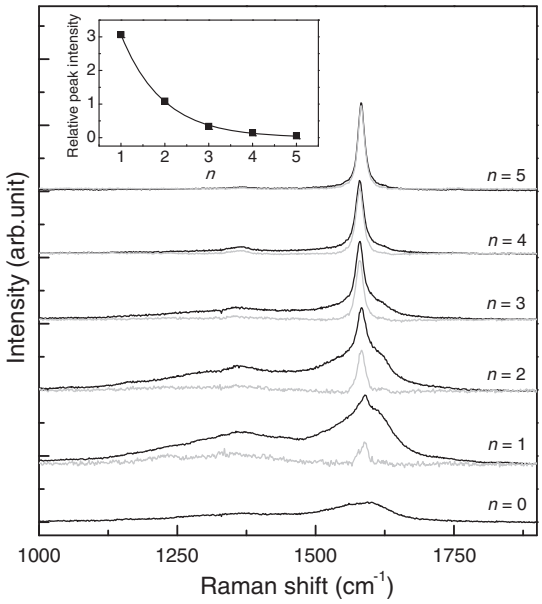

Fig. 3. Evolution of the D and G bands in Ag/graphene as a function of graphene layers number (n). Gray curves denote the G peak component estimated by the spectral analysis (see text). The inset shows the relative intensity of the broad G peak components to the sharp G peak component.

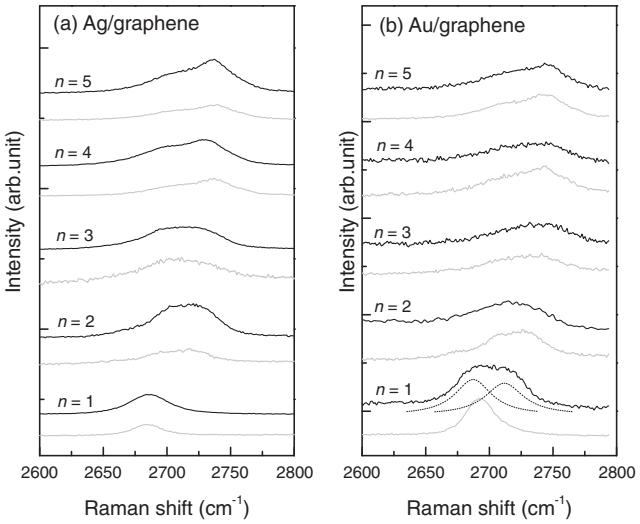

Fig. 4. A pair of the Raman spectra of the (a) Ag/graphene and (b) Au/graphene samples in the 2D band regions. Black curves are from the Ag/graphene and Au/graphene heterostructure regions and gray curves are from the pristine graphene regions with different graphene layers number ($n = 1$–5), respectively.

broadenings compared to those in the corresponding pristine graphene regions. The enhancement of the Raman signals by SERS is also observed in the Ag/graphene heterostructure; the spectral intensity from Ag/single layer graphene (SLG) is 4 times larger than that from pristine SLG. The formation of the heterostructure also causes the significant changes in the spectral features around the D and G band regions. An intense peak ascribed to the D band appears and the D and G bands are broadened remarkably. In case of the Au/graphene heterostructure, on the other hand, the pronounced changes in the Raman spectra are only observed in the 2D band different from Ag/graphene. The G band of Au/graphene also exhibits the peak-broadening, although the extent is much smaller compared with the case in Ag/graphene. In the following, these characteristic features in the G and 2D bands of Ag/graphene and Au/graphene will be discussed in detail.

Figure 3 shows the evolution of the G band Raman signals in the Ag/graphene sample as a function of the number of graphene layers. As mentioned above, the D band appears and the two peaks (D and G bands) are broadened. These broadened features become ambiguous with increasing the number of graphene layers beyond a few layers. It is worthy to note that the similar broadened features can be observed even in the area of Ag/glass ($n = 0$), where no graphene sheet exists, on the Ag/graphene sample. The obtained spectrum from the Ag/glass area coincides well with the one from the distorted graphitic structures.[25] A more detailed analysis has made clear that the D and G bands of Ag/graphene ($n = 1$–5) consists of broad and sharp peak components in the G band and a broad peak in the D band, respectively. Gray lines shown in Fig. 3 are the D- and G-band spectra obtained by approximately subtracting the contribution from the broad components from the raw spectra of Ag/graphene, assuming that the broad components are identical to the Raman spectrum of Ag/glass ($n = 0$). In the inset of Fig. 3, the relative peak-intensity of the broad peak component to the sharp peak component in the G band is plotted as a function of n. The intensity of the broad peak component is found to decrease exponentially with increasing the number of graphene layers. The critical thickness t in an exponential function of $a\exp(-n/t)$ is estimated as $t = 1$, where a is the constant and n is the number of graphene layers. This indicates that the distorted graphitic structure exists at the graphene/glass interface and not at the Ag/graphene interface or in the graphene interlayer. The broad spectral feature could come from the disordered graphitic carbons like small graphene particles which were adhered on the glass surface during the sample preparation by the micromechanical cleavage method. In the Ag/graphene heterostructure, a pronounced signal enhancement by SERS may clarify the existence of disordered graphitic carbons unintentionally generated during the process of the micromechanical cleavage. In the present study, the existence of the disordered graphitic carbons was evaluated at the graphene–glass interface only. From a practical point of view, the evaluation should be further carried out at the other interfaces such as graphene/SiO_2, for plenty of studies of both electronic and spintronic devices have been performed in such system. This is an important subject to be solved for the practical device design. The rather intense broad peak component makes it difficult to analyze the sharp G peak components which would be attributed to the graphene sheet, therefore a comparative discussion about interface interactions at Ag/graphene and Au/graphene will be carried out on the 2D band in the following.

Figure 4 shows the evolutions of the 2D band Raman spectra in the (a) Ag/graphene and (b) Au/graphene samples as a function of the number of graphene layers. In these figures, the data consist of pairs of two spectra obtained at the heterostructure region (black line) and at the pristine

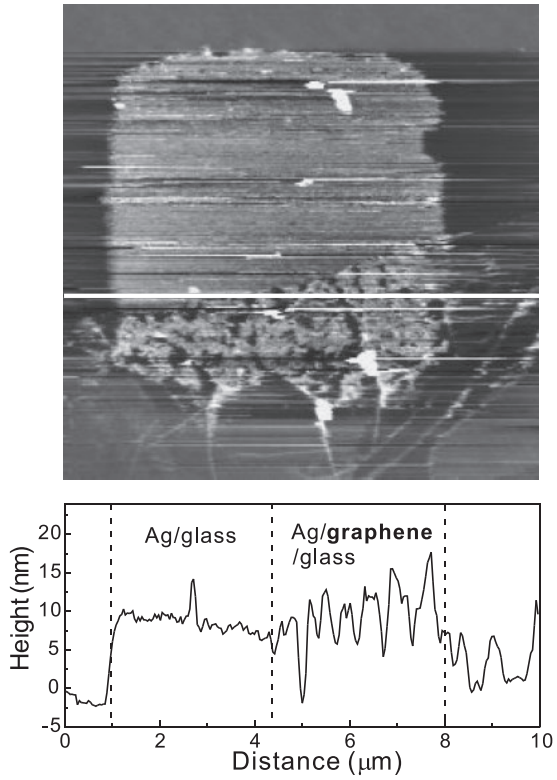

Fig. 5. AFM image of Ag/graphene. A sectional line profile taken along the white line is shown in the lower panel.

graphene region (gray line) with the identical graphene layers number ($n = 1$–5). It is found that, in the heterostructure regions, the respective peaks exhibit the shifts of the peak positions and also the broadenings compared to those in the corresponding pristine graphene regions. These changes are more pronounced in the heterostructures composed of the single–several layer graphenes, and therefore can be attributed to the effect of the metal/graphene interface formation. In Fig. 4(b), the 2D band in the Au/graphene heterostructure region can be separated into two peak components with larger and smaller shifts with respect to the positions of these bands in the pristine graphene, aside from the several peak components originating each 2D band as mentioned above. The two components of the 2D band with larger and smaller shifts observed in the heterostructure region can be assumed to come from the "true" heterostructure region covered with Au and the bare graphene region (two different areas), respectively, because a part of the graphene surface is not covered with Au due to the discontinuous distribution of coarse Au grains. This has been previously mentioned elsewhere.[13] Similarly, the AFM image of Ag/graphene shown in Fig. 5 indicates that the growth mode of Ag is different between on the graphene and on the glass surfaces; a part of the graphene surface is not covered with Ag. However, the two peak components as seen in the 2D band of Au/SLG ($n = 1$) is not identified in the spectrum of Ag/SLG ($n = 1$) (see Fig. 4). This contradictory result could be explained by considering the effect of SERS. Namely, the enhancement of the Raman signal by SERS is expected to occur only in the "true" heterostructure attached with Ag grains. The obtained 2D band signals in Fig. 4(a) is thus considered to come from the Ag/graphene heterostructure. In Fig. 4, no significant shift of the peak positions of the 2D band is observed in between pristine graphene and Ag/graphene, whereas the 2D band shift in Au/graphene exhibits more than $\sim 15\,\mathrm{cm}^{-1}$ at the Au/SLG heterostructure. It has been reported that the interactions at the metal/graphene interface result in the peak shifts of the G and 2D bands. In the transition metal/graphene heterostructures, the covalent-type interaction between transition metal and graphene causes a large peak shift and broadening in the G and 2D bands.[13] These changes are considered to be due to the weakening of the graphene C–C bonds by the occupation of the antibonding π^*-derived states induced by the π–d hybridization at the interface. In the noble metal/graphene heterostructures (Ag, Au/graphene), on the other hand, it has been theoretically demonstrated that the interface interaction is weaker than the transition metal-graphene interface interaction.[12] In these heterostructures with weak interaction, it has been reported that the doping of electrons/holes at the metal/graphene interface also causes peak shifts of the G and 2D bands.[18–20] The amount of the G and 2D peak shift is roughly proportional to the amount of doped carriers.[18,19] The small 2D band shift in Ag/graphene is considered to be due to the small carrier doping at the interface, since the work function difference is relatively small between Ag (4.26 eV) and graphene (~4.6 eV) as compared with that between Au (5.1 eV) and graphene.[26]

4. Conclusions

Interactions of single/multilayer graphene with noble metals were investigated for the metal/graphene heterostructures fabricated by metal deposition onto the microcleaved graphene surface, by using confocal micro-Raman spectroscopy. Precise mesurements of the graphene layers number dependence of the D and G peak features revealed that the disorder graphitic carbons are adhered unintentionally on the glass substrate during the samples preparation by the micromechanical cleavage method. A significant difference in the 2D peak shift arose between Ag/graphene (small shift) and Au/graphene (large shift), which can be explained by the difference in the amount of the doped carriers in graphene between Ag/graphene (small) and Au/graphene (large) related to the work function difference between Ag-graphene (small difference) and Au-graphene (relatively large difference).

Acknowledgments

This work was partly supported by Grants-in-Aid for Scientific Research B (Grant No. 19360290), for Yong Scientists (Start-up) (Grant No. 21860089), and for Yong Scientists B (Grant Nos. 22740206 and 22760033) from the Japan Society for the Promotion of Science.

1) K. S. Novoselov, A. K. Geim, S. V. Morozov, D. Jiang, Y. Zhang, S. V. Dubonos, I. V. Grigorieva, and A. A. Firsov: Science **306** (2004) 666.
2) K. S. Novoselov, A. K. Geim, S. V. Morozov, M. I. Katsnelson, I. V. Grigorieva, S. V. Dubonos, and A. A. Firsov: Nature **438** (2005) 197.
3) Y. Zhang, Y.-W. Tan, H. L. Stormer, and P. Kim: Nature **438** (2005) 201.
4) H. B. Heersche, P. Jarillo-Herrero, J. B. Oostinga, L. M. K. Vandersypen, and A. F. Morpurgo: Nature **446** (2007) 56.
5) S. Sakai, I. Sugai, S. Mitani, K. Takanashi, Y. Matsumoto, H. Naramoto,

P. V. Avramov, S. Okayasu, and Y. Maeda: Appl. Phys. Lett. **91** (2007) 242104.
6) Y. Matsumoto, S. Sakai, Y. Takagi, T. Nakagawa, T. Yokoyama, T. Shimada, S. Mitani, K. Takanashi, H. Naramoto, and Y. Maeda: Chem. Phys. Lett. **470** (2009) 244.
7) A. Nagashima, N. Tejima, and C. Oshima: Phys. Rev. B **50** (1994) 17487.
8) K. Yamamoto, M. Fukushima, T. Osaka, and C. Oshima: Phys. Rev. B **45** (1992) 11358.
9) A. Varykhalov, J. Sánchez-Barriga, A. M. Shikin, C. Biswas, E. Vescovo, A. Rybkin, D. Marchenko, and O. Rader: Phys. Rev. Lett. **101** (2008) 157601.
10) A. M. Shikin, G. V. Prudnikova, V. K. Adamchuk, F. Moresco, and K.-H. Rieder: Phys. Rev. B **62** (2000) 13202.
11) D. Farías, A. M. Shinkin, K.-H. Rieder, and Y. S. Dedkov: J. Phys.: Condens. Matter **11** (1999) 8453.
12) G. Giovannetti, P. A. Khomyakov, G. Brocks, V. M. Karpan, J. van den Brink, and P. J. Kelly: Phys. Rev. Lett. **101** (2008) 026803.
13) S. Entani, S. Sakai, Y. Matsumoto, H. Naramoto, T. Hao, and Y. Maeda: J. Phys. Chem. C **114** (2010) 20042.
14) D. Graf, F. Molitor, K. Ensslin, C. Stampfer, A. Jungen, C. Hierold, and L. Wirtz: Nano Lett. **7** (2007) 238.
15) Y. Y. Wang, Z. H. Ni, T. Yu, Z. X. Shen, H. M. Wang, Y. H. Wu, W. Chen, and A. T. S. Wee: J. Phys. Chem. C **112** (2008) 10637.
16) A. C. Ferrari, J. C. Meyer, V. Scardaci, C. Casiraghi, M. Lazzeri, F. Mauri, S. Piscanec, D. Jiang, K. S. Novoselov, S. Roth, and A. K. Geim: Phys. Rev. Lett. **97** (2006) 187401.
17) A. C. Ferrari and J. Robertson: Phys. Rev. B **61** (2000) 14095.
18) J. Yan, Y. Zhang, P. Kim, and A. Pinczuk: Phys. Rev. Lett. **98** (2007) 166802.
19) S. Pisana, M. Lazzeri, C. Casiraghi, K. S. Novoselov, A. K. Geim, A. C. Ferrari, and F. Mauri: Nat. Mater. **6** (2007) 198.
20) A. Das, B. Chakraborty, S. Piscanec, S. Pisana, A. K. Sood, and A. C. Ferrari: Phys. Rev. B **79** (2009) 155417.
21) S. Piscanec, M. Lazzeri, F. Mauri, A. C. Ferrari, and J. Robertson: Phys. Rev. Lett. **93** (2004) 185503.
22) M. Lazzeri and F. Mauri: Phys. Rev. Lett. **97** (2006) 266407.
23) C. Casiraghi, S. Pisana, K. S. Novoselov, A. K. Geim, and A. C. Ferrari: Appl. Phys. Lett. **91** (2007) 233108.
24) K. S. Novoselov, D. Jiang, F. Schedin, T. J. Booth, V. V. Khotkevich, S. V. Morozov, and A. K. Geim: Proc. Natl. Acad. Sci. U.S.A. **102** (2005) 10451.
25) B. J. Nemanich and S. A. Solin: Phys. Rev. B **20** (1979) 392.
26) H. B. Michaelson: J. Appl. Phys. **48** (1977) 4729.